

Combined Fluid Loop Thermal Management for Electric Drive Vehicle Range Improvement

Daniel Leighton
National Renewable Energy Laboratory

ABSTRACT

Electric drive vehicles (EDVs) have complex thermal management requirements not present in conventional vehicles. In addition to cabin conditioning, the energy storage system (ESS) and power electronics and electric motor (PEEM) subsystems also require thermal management. Many current-generation EDVs utilize separate cooling systems, adding both weight and volume, and lack abundant waste heat from an engine for cabin heating. Some use battery energy to heat the cabin via electrical resistance heating, which can result in vehicle range reductions of 50% under cold ambient conditions. These thermal challenges present an opportunity for integrated vehicle thermal management technologies that reduce weight and volume and increase cabin heating efficiency.

Bench testing was conducted to evaluate a combined fluid loop technology that unifies the cabin air-conditioning and heating, ESS thermal management, and PEEM cooling into a single liquid coolant-based system. This system has separate hot and cold fluid streams that are directed to the thermal components as required. The advantages include PEEM waste heat recovery to supplement cabin heating and heat pump operation without refrigerant cycle reversal. A bench test apparatus was constructed to apply transient drive cycle loads to the thermal system and measure the performance under ambient temperatures from -12°C to 43°C . The system proved capable of meeting component thermal requirements at all tested conditions. Furthermore, the system demonstrated a 9% range increase on a nationally weighted basis that accounts for vehicle usage and ambient temperature. The range improvement is expected to be greater for an optimized in-vehicle system.

CITATION: Leighton, D., "Combined Fluid Loop Thermal Management for Electric Drive Vehicle Range Improvement," *SAE Int. J. Passeng. Cars - Mech. Syst.* 8(2):2015, doi:10.4271/2015-01-1709.

INTRODUCTION

Relative to traditional internal combustion engine vehicles, electric-drive vehicles (EDVs) have increased vehicle thermal management complexity through the addition of a battery pack, also known as the energy storage system (ESS), as well as power electronics and electric motor (PEEM) components. These drivetrain subsystems have specific thermal requirements that have necessitated a separate thermal loop for each subsystem. The ESS must be cooled during hot ambient conditions to prevent degradation of battery cell life and must be heated during cold ambient conditions to enable adequate discharge power. The typical range of temperature control for the ESS battery cells is 15°C to 35°C [1]. The PEEM systems must be cooled so that they remain below their maximum operating temperature limits to prevent thermal damage or failure. The typical thermal limits for the PE and EM components are around 150°C [2, 3].

Separate cooling loops typically entail additional heat exchangers at the front end of the vehicle, water/ethylene glycol (WEG) coolant, piping, and WEG pumps. The disadvantage of multiple cooling loops is that they increase vehicle weight, aerodynamic drag, and fan/pump power, thus reducing EDV range. Due to the lack of abundant engine waste heat that is typically available in traditional vehicles, EDVs also suffer from significant range loss when heating the cabin in cold

weather conditions. Cold-weather range loss can be as high as 50% [4], which reduces customer acceptance of EDVs by increasing range anxiety, and presents a barrier for the penetration of EDVs into the national vehicle fleet. The goal of the combined fluid loop (CFL) technology is to improve EDV range and reduce thermal system weight and volume by capturing the synergistic benefits of unifying the thermal management systems.

The CFL technology being investigated unifies the cabin, ESS, and PEEM thermal management into a single coolant-based system with separate hot and cold fluid streams that are directed to the thermal components as required. The unified system has a single heat exchanger at the front end of the vehicle that either rejects or absorbs heat based on the CFL system's operating mode. The design of the system piping allows the coolant to be directed based on operating requirements, including actively heating or cooling the ESS, using the high-temperature coolant stream to cool the PEEM, and recovering the waste heat from the PEEM to supplement cabin heating. The CFL system also enables hot or cold coolant to be directed to the passenger cabin, which means that the system can act as either an air-conditioner or heat pump without reversing the refrigerant cycle. This is advantageous because refrigerant cycle reversal induces refrigerant charge and oil migration issues, as well as

requiring the heat exchangers to act as both condensers and evaporators depending on the operating mode. This dual usage of the heat exchanger makes heat exchanger design more difficult because performance trade-offs must be made so that the heat exchangers perform adequately in both operating configurations rather than optimizing each for a single application.

It is expected that the CFL system will increase cold-weather EDV range by minimizing electrical resistance heating of the cabin through recovery of PEEM waste heat and heat pump operation. Minimizing the area and number of heat exchangers at the front end of the vehicle has the potential to reduce the aerodynamic drag of the vehicle. An additional benefit of combining fluid loops is that the ESS, passenger compartment, and thermal management fluid loops can be preconditioned when the vehicle is connected to grid power.

APPROACH

Feasibility Study

Using component bench data, National Renewable Energy Laboratory (NREL) researchers conducted an initial feasibility study to predict CFL thermal performance through software simulation. The key results of this study were that the ESS and PEEM thermal demands could be met using a combined approach without significant impact on cabin conditioning [5]. This is an important finding because CFL technology must be capable of maintaining the PEEM component temperatures below the required limits using the hot coolant circuit instead of the cold coolant circuit, which would have a large negative impact on cabin cooling capacity. After determining feasibility through simulation, an experimental bench test system was constructed using available prototype components to validate the simulation findings and measure thermal system performance for cooling and heating conditions. Although sufficient for bench testing, it is expected that the prototype components could be further optimized for improved system capacity and efficiency.

Bench Test Apparatus

To perform the experimental study, a bench test apparatus capable of evaluating the steady-state and transient performance of EDV thermal systems was constructed. The purpose of the test apparatus is to measure the impact of the CFL technology on EDV range. The test apparatus is a hardware-in-the-loop system that imposes actual thermal loads on the experimental system and measures the resulting energy consumption and thermal performance. To impose realistic EDV loads on the thermal system, the test bench incorporates a vehicle powertrain model, thermal and efficiency PEEM and ESS models, and a thermal cabin model. The model-based portions of the bench test apparatus are adapted into a control and data acquisition LabVIEW program for continuous feedback based on thermal system performance. The vehicle powertrain model is a LabVIEW adaptation of NREL's power-based FASTSim model [6], the PEEM and ESS models are based on the previous NREL CFL simulation work [5], and the cabin model is from prior work by Gado [7]. The PEEM, ESS, and cabin models are all lumped capacitance physics-based models. Some of the basic parameters of the models are given in Table 1.

Table 1. Selection of basic model inputs

Vehicle type	Mid-sized battery electric vehicle
Battery capacity	24 kWh
Usable state of charge range	90%
Maximum powertrain power	80 kW
ESS mass (including housing)	348 kg

The physical bench test apparatus consists of two separate air ducts, a cabin air simulator, and an outdoor air simulator, as shown schematically in Figure 1. The cabin air simulator recreates the conditions seen inside of the heating, ventilation, and air-conditioning (HVAC) module in the instrument panel of a vehicle, and therefore houses the experimental system's heater core and cooler core heat exchangers. It can achieve air flow rates up to 425 m³/hr. and can simulate temperatures from -30°C to 63°C. The outdoor air simulator recreates the conditions seen by the heat exchangers at the front end of the vehicle, and therefore houses the front end heat exchanger of the experimental system. It is capable of air flow rates up to 3,400 m³/hr and can simulate temperatures from -30°C to 43°C. The airflow rate is continuously scaled based on the simulated vehicle speed to capture the effect of vehicle ram air on heat exchanger performance. To simulate a given ambient temperature condition, the test apparatus draws in fresh air from the laboratory and heats it to the control temperature. The bench test apparatus is not capable of actively cooling the intake airstream and therefore must always be operated in an environment that is at a lower temperature than the simulated ambient temperature.

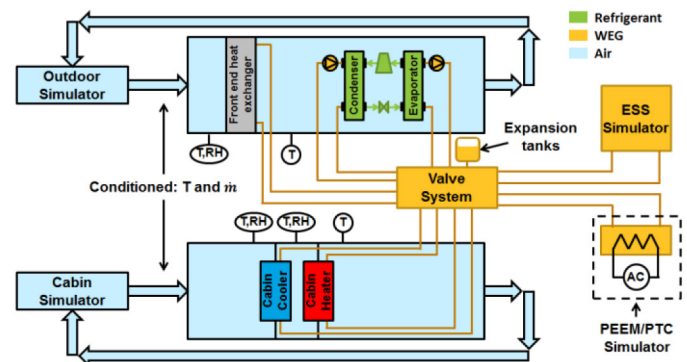


Figure 1. Basic schematic of CFL bench test apparatus

The bench test apparatus has two electrical resistance coolant heaters, one to simulate the heat from the vehicle PEEM and supplemental heat from the positive temperature coefficient (PTC) electrical resistance heater; and the other to simulate the heat from the hot-soaked ESS. The ESS simulator also has a coolant-to-air heat exchanger that can reject heat to the ambient laboratory air when simulating the thermal load of a cold-soaked ESS. The coolant outlet conditions from the PEEM and ESS components were predicted with the software models for a virtual vehicle and imposed on the actual experimental system with the coolant heaters. In the model, the full coolant mass flow rate passes through the PE before subsequently passing through the EM; however, this is imposed on the experimental system as a single coolant load. A picture of the assembled bench test apparatus is shown in Figure 2.



Figure 2. CFL bench test apparatus. Photo by Daniel Leighton, NREL.

Experimental CFL System

The experimental CFL system was constructed with six heat exchangers and a thermostatic expansion valve (TEV) provided by Delphi. The heat exchangers included a production radiator as the front-end heat exchanger, a production heater core, a prototype cooler core that was a coolant-to-air heat exchanger used to cool the cabin, a prototype plate-type evaporator, a prototype plate-type condenser, and a prototype plate-type sub-cooler. To complete the system a prototype electric automotive compressor was provided by Halla Visteon Climate Control. The electric compressor was powered with a high-voltage direct current (DC) power supply that simulated the power provided by an EDV traction battery pack. The compressor was a variable speed scroll-type, and the refrigerant used was R-134a. The refrigerant system components are shown in Figure 3.

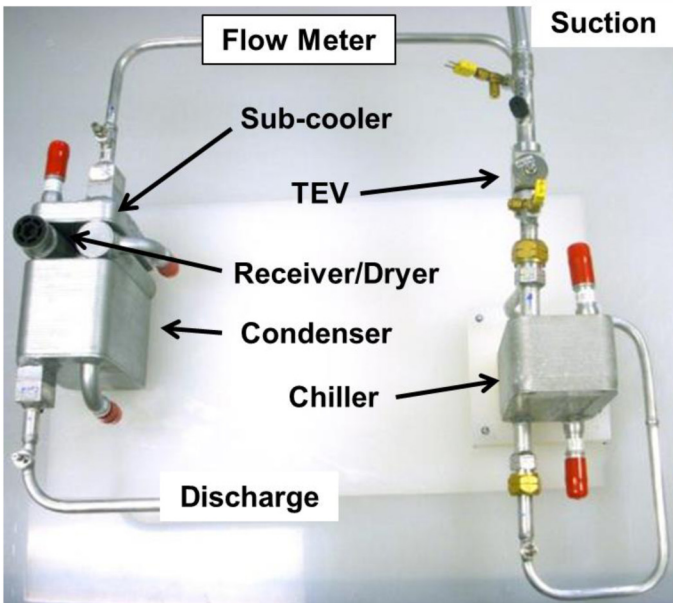


Figure 3. Delphi prototype refrigerant system components. Photo by Daniel Leighton, NREL.

The flow path of the refrigerant system was configured so that low-temperature, low-pressure vapor is compressed by the compressor to a high-temperature, high-pressure vapor. The refrigerant vapor then passes through the condenser, where it rejects heat and condenses to a high-pressure liquid before passing through the sub-cooler where further heat is rejected to achieve a sub-cooled liquid. The liquid is then expanded through a TEV to a low-pressure, low-temperature two-phase refrigerant that is passed through the evaporator to absorb heat and vaporize the remaining liquid. The low-temperature, low-pressure vapor then completes the circuit back to the compressor.

The experimental system used a 50%/50% mixture of water and ethylene glycol by weight as the coolant working fluid. The coolant circuit was formed with 3/4-in. inner diameter automotive radiator hose, with two automotive 12-V direct current electric coolant pumps that separately pumped the hot and cold fluid loops. The coolant pumps were operated at full speed for all test conditions and consumed approximately 60 watts each. The flow rate of the pumps depended on the pressure drop of the operating configuration and the coolant temperature for each given test condition. The volumetric flow rate of the pumps varied from approximately 8 L/min to 14 L/min. Laboratory-grade ball valves were used to control the circuit flow paths and to provide variable bypass capability of the heat exchangers. The experimental system piping and valving arrangement was designed to allow maximum flexibility for experimental bench testing, and is not representative of the configuration expected for in-vehicle applications. A schematic of the fully assembled experimental system is shown in Figure 4.

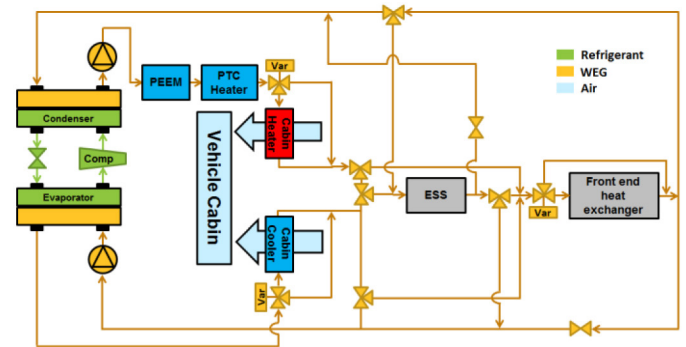


Figure 4. Schematic of full experimental CFL system

The experimental CFL system piping and valving design allows for a number of test configurations, including cooling of the PEEM and ESS systems when the compressor is deactivated by using the ambient air as a heat sink via the front-end heat exchanger. For the purposes of this study, there are two main configurations of interest that can be used to judge the energy efficiency of the system-cooling mode and heating mode. In the cooling mode configuration, the hot-side coolant sequentially absorbs heat from the condenser, absorbs heat from the PEEM systems, rejects heat through the front-end heat exchanger, and finally completes the hot circuit back to the condenser. On the cold-circuit side, the coolant sequentially rejects heat to the evaporator, absorbs heat from the cabin, absorbs heat from the ESS, and completes the cold circuit back to the evaporator. This configuration enables cabin air-conditioning (A/C),

approached the blower speed will reduce, which will lower the heating capacity required to maintain the 50°C vent outlet set point. In extremely cold conditions, the heat pump capacity is low and the heating load of the cabin is high, necessitating the continuous operation of the supplemental PTC heater at partial capacity in addition to the compressor at full speed to maintain cabin comfort. The cabin heater core inlet air temperature recirculation damper control is set to 15%/85% outside/recirculated air for the entire duration of all of the heating mode tests.

When active cooling of the ESS was needed for hot ambient conditions, a simple on/off coolant flow control thermostat was used. The flow control thermostat was implemented as a virtual model rather than actual valve and pipe within the test apparatus to enable maximum flexibility. Therefore, 100% of the actual WEG coolant flow always passed through the ESS simulator, but the effect on the outlet conditions controlled by the model was adjusted according to the control strategy. This controller allowed 10% of the total WEG coolant mass flow to pass through the ESS when in the “on” configuration, and 0% of the total WEG coolant mass flow rate to pass through the ESS when in the “off” configuration. It was desirable to maintain the ESS temperature between 15°C and 35°C; therefore the cooling mode thermostat was set to 32.5°C with a 2.5°C band. This thermostat control allowed the ESS to be conditioned to the desired upper temperature limit for longevity, but minimized the load on the compressor to maximize vehicle range. The thermal mass of the ESS was large enough so that the cycle time of the thermostat due to self-heating of the battery under load was long. In fact, after initial cool-down of the battery the thermostat did not cycle back on within the durations of the drive cycles tested. When active heating of the ESS was required to maintain adequate power output performance, the thermostat was set to heat with 10% coolant flow until the ESS temperature was above 15°C. After being warmed to 15°C, self-heating of the ESS under load maintained the temperature for the remainder of the drive cycles tested. Because the battery model was a lumped-capacitance model instead of a cell-level model, issues of non-uniformity among cell temperatures were not considered. The control scheme was designed to be simple and repeatable and is therefore only representative of the potential impact of ESS thermal management. The actual impact of ESS thermal management will vary significantly depending on the vehicle implementation and control design.

To predict the impact of the CFL technology on EDV range, realistic transient test conditions need to be imposed. Transient operation is vital for accurately capturing the effects on the thermal subsystems such as the cabin, PEEM, and ESS. This is particularly true for determining whether or not the CFL system can adequately condition the PEEM components using the hot coolant stream. In terms of energy consumption, a key aspect of transient testing is the duration of the test as this will dictate the weighted effect of the transient cabin cool-down/warm-up loads versus the steady-state cabin comfort maintaining loads.

In the United States, the average commute travel time is 22.85 minutes [8]. This is a relatively short duration, which heavily weights transient cabin conditioning for hot- or cold-soaked vehicles. To most accurately predict the impact of the CFL system on vehicle range, it

was desirable to select drive cycles that closely matched this duration. There are also significant differences in vehicle power output and therefore PEEM and ESS thermal demands, between continuous highway driving and stop-and-go city driving. The method used to measure vehicle efficiency was a 45%/55% weighting of the Urban Dynamometer Driving Schedule (UDDS) city cycle and the Highway Fuel Economy Test (HWFET) highway cycle. With a duration of 22.9 minutes, the UDDS cycle almost exactly matches the average commute travel time. When the HWFET cycle is doubled by running two full cycles back-to-back, the total duration is 25.5 minutes, which is sufficiently close to the average commute. A plot of vehicle speed versus time for the two drive cycles used is shown in Figure 7.

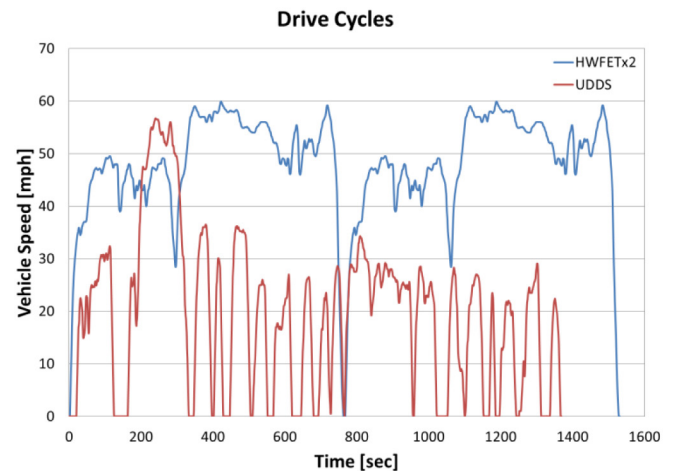


Figure 7. Drive cycle profiles for UDDS and double HWFET

RESULTS

Cooling

Cooling mode in the experimental investigation is considered to be the simulated ambient temperature test conditions from 23°C to 43°C in increments of 5°C. In addition to the heat transfer between the ambient air and cabin air calculated by the cabin model, all of the cooling mode tests also included a 1-kW solar load imposed on the cabin air to simulate high, but realistic solar loading of a south-facing mid-sized vehicle. All of the test conditions also included a single passenger, which is simulated as a 100-W internal cabin load. “Soak” test cases simulated a cabin that was hot soaked in the sun while facing south on a clear solar day. The simple input parameter is that the average cabin air and average interior mass temperatures were uniformly 20°C above the ambient temperature at the start of all soak test cases, a realistic value based on experimental vehicle testing results. The coolant and refrigerant system temperatures started at the ambient temperatures for the soak cases rather than the elevated soaked cabin temperature. The soak test cases were used to measure the impact of hot soaking the vehicle on the CFL system performance and subsequently the vehicle range. The humidity of the air in the test apparatus was low enough so that the cooler core did not accumulate water vapor condensation under any of the test conditions.

One of the major findings of the cooling mode testing was that the PEEM component temperatures were kept well within the 150°C limitation for all of the ambient temperatures tested when using the

hot coolant stream to remove PEEM waste heat. The maximum instantaneous temperature observed during any of the cooling mode conditions tested was less than 100°C for the PE and 90°C for the EM. Example component temperatures are shown in Figure 8 for a double HWFET drive cycle at an ambient temperature of 38°C.

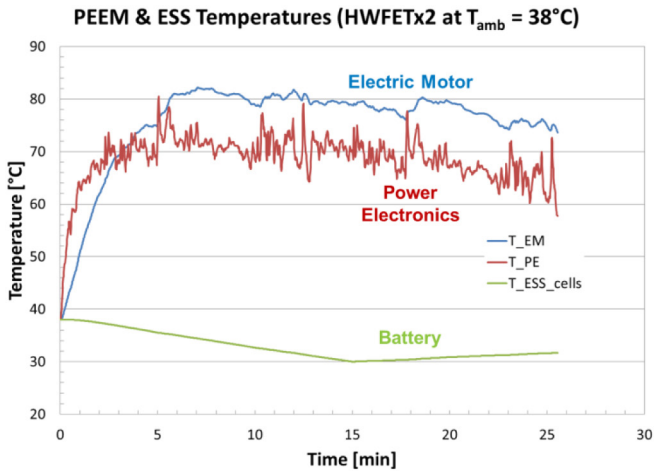


Figure 8. Component temperatures for cooling mode, double HWFET cycle, $T_{amb} = 38^{\circ}\text{C}$, no soak, PEEM and ESS cooling case

The data demonstrate the rapidly fluctuating PE temperature due to its relatively low thermal mass, which necessitates continuous cooling to avoid rapidly exceeding its thermal limits. The EM temperature fluctuates more slowly than the PE because of the larger thermal mass, but the transient nature of the drive cycle powertrain system load can still be observed. The ESS has a very large thermal mass; because of this, it is apparent that the average ESS temperature is independent of the changing power load and is more closely related to the cooling capacity and starting temperature. This indicates that the ESS is the component that would benefit most from thermal pre-conditioning. Approximately 15 minutes into the drive cycle, the ESS thermostat control cycles off the coolant flow to the ESS. The effect of removing the ESS thermal load from the cooling system can be observed in the cabin cooling rate as demonstrated in Figure 9 for the same test.

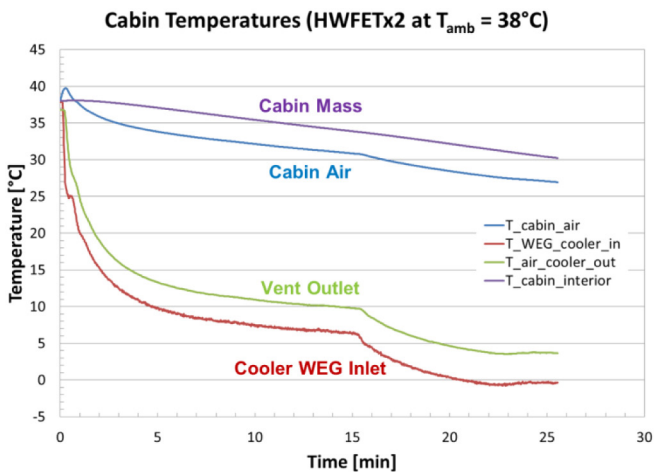


Figure 9. Cabin temperatures for cooling mode, double HWFET cycle, $T_{amb} = 38^{\circ}\text{C}$, no soak, PEEM and ESS cooling case

At the beginning of the test, it can be observed that the cabin and cooling system started at an initial temperature equal to the ambient temperature, and then began to cool down when the compressor started. The slight increase in cabin air temperature at the start was due to the sudden solar load on the non-solar soaked vehicle. Essentially this is representing the cabin behavior if the vehicle was parked in the shade and then driven into the direct sun at time zero of the drive cycle. The air temperature increases because the solar load exceeds the A/C cooling capacity for the first 30 seconds of the test. When the ESS thermostat control turns the coolant flow off after 15 minutes, the compressor cooling capacity is able to control the vent outlet temperature to 3°C, which maximizes the rate of cabin cooling.

An observation of the experimental testing is that the experimental system thermal mass was larger than a realistic implementation of an in-vehicle system. This is due to the larger number of laboratory-grade valves, additional piping and WEG coolant, sensors, and other thermally massive components necessary for experimental testing. The consequence of the larger thermal mass is that the cooling system capacity to the cabin is lower than it would be in an actual vehicle system, resulting in a longer cool-down period, which requires additional compressor energy consumption. This was deemed acceptable for the purposes of concept bench testing, but it is expected that an actual vehicle system would have superior performance and energy efficiency.

Eight drive cycle tests were conducted for each cooling mode ambient temperature, with four unique test configurations that were each tested with the UDDS and double HWFET drive cycles. The first test quantified the energy consumption of operating just the A/C system without conditioning the PEEM or ESS systems, shown as the “A/C Penalty” in Figure 10. This represented the performance of a secondary loop A/C system that does not utilize the CFL integration technology. The second test included PEEM cooling to measure the impact on A/C performance. The third test added ESS cooling to the PEEM cooling, to measure the energy consumption of using active ESS cooling. The final test included all of the above conditions in addition to a hot-soaked cabin to measure the sensitivity of the system performance to initial cabin temperature. The total possible range of the vehicle if the A/C, ESS cooling, and PEEM cooling were not operated is represented by the summation of the data bars for a given ambient temperature in Figure 10.

As expected, the cabin A/C energy consumption, or “A/C Penalty,” increased with increasing ambient temperature. This reflects the additional compressor power required for higher condenser pressures at higher ambient temperatures as well as the longer runtimes of the compressor at maximum speed during higher temperature cabin cool-downs. The vehicle range loss due to cabin A/C varies from 9.6% for mild cooling to 37.3% at the highest ambient temperatures. The additional load of PEEM cooling on the CFL system was negligible for ambient temperatures of 28°C or less. For higher temperatures, the maximum range loss due to PEEM cooling is only 1.4%, and is less than 1% at the highest ambient temperatures. This loss is due to the slightly increased condenser pressure due to the elevated temperature of the hot coolant loop. ESS cooling was only activated by the thermostat control systems at the tested ambient

temperatures of 33°C and above and therefore had no impact on range at lower temperatures. The range loss due to ESS conditioning increased with increasing ambient temperature up to 2.8% at the highest ambient temperatures. This is a moderate impact on range, but necessary in order to condition the ESS for longevity.

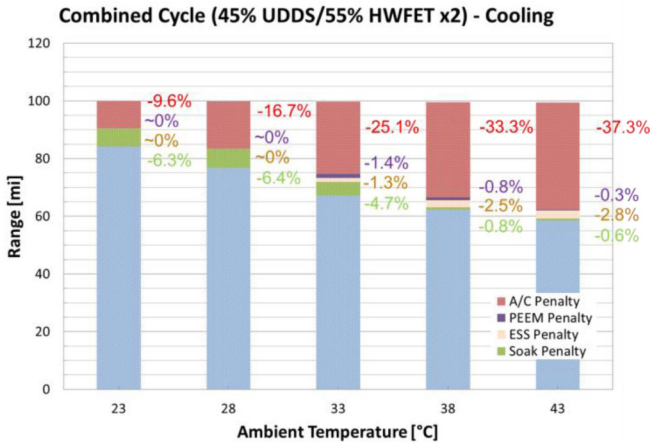


Figure 10. Summary of combined drive cycle cooling results for vehicle range

The impact of a hot-soaked cabin on the A/C energy consumption is significant due to the longer period of full speed compressor operation required for cool-down to cabin comfort. The reduction in vehicle range is as high as 6.4% for ambient temperatures below 38°C. For the 38°C and 43°C cases, the effect is less than 1% due to the control strategy and system sizing. For cases below 38°C, the cabin temperature reaches the 25°C set point within the duration of the drive cycle, but in the hotter ambient temperature cases without soak the cabin never reaches comfort temperature within the drive cycle duration, as demonstrated in Figure 9. The consequence is that there is not a significant difference in energy consumption when compared with the soaked case because the compressor operates at maximum speed for the entire duration of both cases. The small increase in energy consumption of the soaked case is because of the slightly higher average cabin cooler inlet air temperature. The higher average inlet temperature is due to the recirculation mode control engaging later in the drive cycle because it takes longer for the cabin air temperature to drop below the ambient temperature.

Heating

Heating mode for the experimental investigation is considered to be the simulated ambient temperature test conditions below 23°C in increments of 5°C. All of the test conditions included a single passenger, which is simulated with a 100-W internal cabin load. The heating mode tests assume zero solar loading on the cabin to simulate a severe heating case. Solar “soak” test cases were not conducted, and the cabin air, cabin mass, coolant, and refrigerant system temperatures were set to the ambient temperature at the start of the tests. The cabin air damper setting remained in recirculation mode (85% recirculation/15% fresh) for the duration of all of the drive cycle tests. Supplemental PTC heating was used for ambient temperatures of 8°C or lower. The humidity of the air in the test apparatus was low enough so that the front-end heat exchanger did not accumulate frost under any of the test conditions.

One of the major findings of the heating mode testing was that the PEEM component temperatures were kept well within the 150°C limitation for all of the ambient temperatures tested when using the hot coolant stream to recover PEEM waste heat. The maximum instantaneous temperature observed during any of the heating mode conditions tested was less than 80°C for the PEEM components. Examples of the component and cabin temperatures for a UDDS drive cycle at an ambient temperature of -2°C are shown in Figure 11 and Figure 12, respectively.

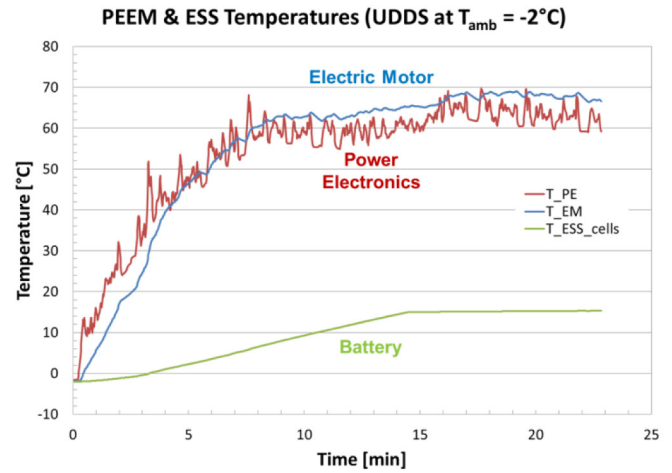


Figure 11. Component temperatures for heating mode, UDDS cycle, $T_{amb} = -2^\circ\text{C}$, PEEM and ESS conditioning case

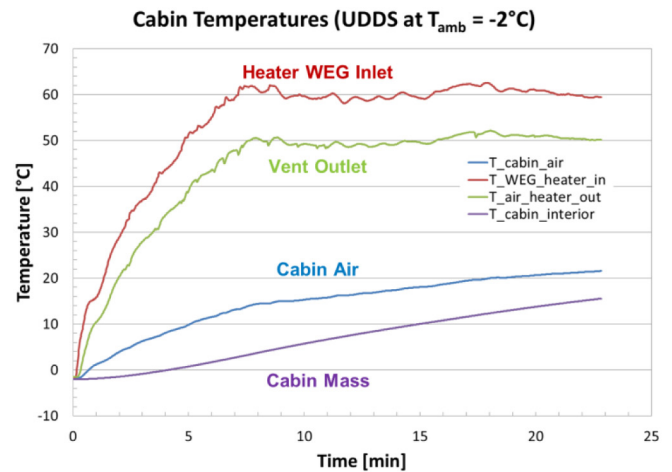


Figure 12. Cabin temperatures for heating mode, UDDS cycle, $T_{amb} = -2^\circ\text{C}$, PEEM and ESS conditioning case

It is apparent that the warm-up rate of the hot-side coolant at the heater core inlet and the PEEM components is similar. This is an expected result, as they are thermally linked by the hot coolant loop. For the first 3.5 minutes of the drive cycle, the EM does not contribute waste heat for cabin heating as the initial waste heat is used to self-heat the thermal mass of the motor. The thermal mass of the PE is small enough so that it contributes waste heat at the start of the cycle. After the target vent outlet air temperature control point is reached at 7.5 minutes the supplemental PTC heating is reduced. Another notable result is that the ESS is actively heated until 14 minutes into the drive cycle when it reaches its 15°C control point. Once the thermostat control system deactivates active ESS heating,

the ESS self-heats slightly during the remainder of the drive cycle. A consequence of the ESS thermostat cycling off is that the total required heating load decreases, which reduces the supplemental PTC heating to zero and allows a reduction in the compressor speed control. This effect is shown in Figure 13.

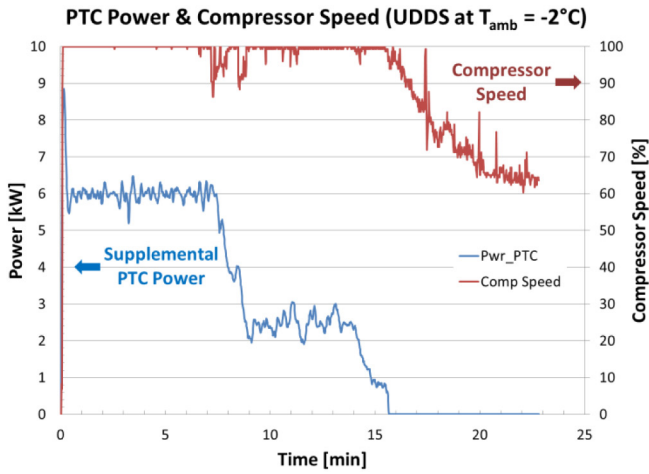


Figure 13. Supplemental PTC heating power and compressor speed for heating mode, UDDS cycle, $T_{amb} = -2^{\circ}\text{C}$, PEEM and ESS conditioning case

Four drive cycle tests were conducted for each heating mode ambient temperature, with two unique test configurations that were each tested with the UDDS and double HWFET drive cycles. The first test consisted of heating the cabin and ESS using the heat pump system without PEEM waste heat recovery, shown as the “HP” case in Figure 14. From this test, the equivalent thermal performance of a PTC-based heating system was derived by assuming a 100% efficient PTC heater that output the same heating capacity as the heat pump system. This was done to ensure that the warm-up performance of the baseline PTC heating case matched the heat pump case, and so that the energy consumption of the PTC heating case could be calculated without requiring an additional experimental test. This is shown as the “PTC Only” case in Figure 14, and it represents the performance of a PTC coolant heater system that does not utilize the CFL integration technology, but does provide active ESS heating. The second test added PEEM waste heat recovery to the heat pump to measure the performance of the fully integrated CFL system. The total possible range of the vehicle if the cabin heating, ESS heating, and PEEM waste heat recovery were not operated is represented by the summation of the data bars for a given ambient temperature in Figure 14.

As expected, the vehicle range decreased with decreasing temperature because the heating system energy consumption increases as the temperature decreases. This is predominantly due to the increasing transient and steady-state vehicle heating loads. For PTC-only heating, the vehicle range loss varies from 28.3% at an ambient temperature of 18°C , to 53.8% at an ambient temperature of -12°C . When operating the heat pump system, the recovered vehicle range varies from 12.8% at 18°C to 1.1% at -12°C . This shows that the heat pump system provides a very large energy efficiency benefit for mild heating conditions, but becomes ineffective at extremely low temperatures. This is due to the decreasing heat pump capacity as the

suction pressure decreases with decreasing ambient temperature. One possible way to improve the low temperature performance would be to use a larger capacity compressor to offset more of the supplemental PTC heating. Under all of the tested conditions, the PEEM waste heat recovery benefit to vehicle range was around 1.5% to 2%. This is a moderate benefit when compared with the heat pump at mild temperatures, but it remains relatively consistent even at the lowest temperatures, making it a valuable contribution. An in-vehicle application of the CFL technology would have a lower thermal mass on the coolant side compared with the experimental system. This would be achieved through a reduction in pipe length, number of valves and sensors, and coolant volume, which would improve cold weather performance by decreasing the supplemental PTC heating needed during warm-up.

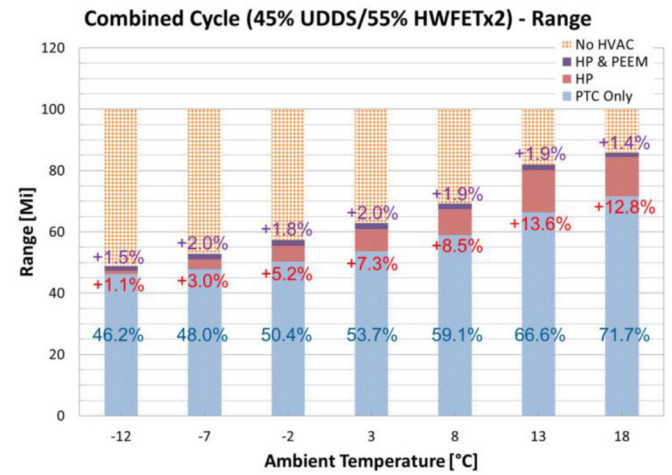


Figure 14. Summary of combined drive cycle heating results for vehicle range

One of the important findings of the cold weather testing is that the heat pump system was only effective down to a minimum temperature of -12°C . For ambient temperatures colder than -12°C , the suction pressure was below atmospheric pressure, creating possible issues of air entrainment in the refrigerant cycle. At ambient temperatures this low the heating capacity of the heat pump system is reduced to a point at which the benefit is approaching zero. For an in-vehicle application, vehicle usage at extreme low temperatures (below -12°C) would necessitate using only the supplemental PTC heater as a source for cabin and ESS heating. PEEM waste heat recovery could still be applied at these extremely low temperature conditions, although the benefit will be reduced due to the cold-soaked EM mass at the start of the drive cycle. One option to improve the extreme cold weather performance would be to switch from a TEV to an electronic expansion valve (EEV). Due to the physics of a TEV, it is difficult to design a valve that is capable of maintaining the desired 5°C of superheating at a wide range of suction pressures that include A/C and heat pump mode. The experimental bench testing showed that the TEV superheat can approach 10°C during operation at an ambient temperature of -12°C . This causes the suction pressure to be lower than desired, which decreases the performance of the compressor. An EEV can be software-tuned so that it does not have this limitation.

Annual Weighting

To accurately predict the impact of the CFL system technology on EDV range at a national level, the measured performance needed to be compared to real world usage data. A study conducted by Duthie took into account the national geographical population distribution, temporal usage data, and weather conditions for light-duty vehicles in the United States [9]. These data were used to weight vehicle usage versus ambient temperature to determine the weighted average effects of CFL system efficiency at various temperatures. Percentage-based vehicle usage versus ambient temperature data are shown in Figure 15.

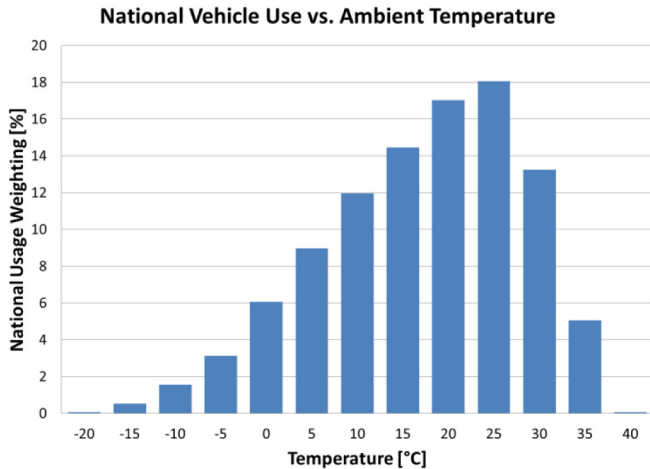


Figure 15. National vehicle use weighting for ambient temperature

It is apparent from the usage data that the majority (>80%) of driving is done in moderate climate conditions, from 5°C to 30°C. The usage data also show that the extreme hot case tested at 43°C represents a very small fraction of the population. Testing revealed that the CFL heat pump operation could not extend below -12°C, but the weighted data extend to -20°C. To account for this extreme cold weather usage, it was assumed that the heat pump would be deactivated for conditions colder than -12°C and instead the supplemental PTC heating would provide 100% of the heating capacity. These assumptions were used to extrapolate system performance down to -20°C. The error introduced on the final result by the extrapolation is negligible because the usage weighting at these temperatures is on the order of 1%.

To compare the CFL system to the standard secondary loop system used as a baseline, the data from Figure 10 and Figure 14 were combined to represent the performance for the entire tested temperature range. The baseline system represents A/C only in cooling mode, meaning that PEEM and ESS cooling are not included. In heating mode, the baseline system does include ESS heating in addition to cabin heating, but does not include PEEM waste heat recovery and uses only supplemental PTC heating, not heat pumping. The CFL system includes ESS and PEEM cooling in cooling mode and PEEM waste heat recovery, ESS heating, and heat pumping in heating mode. In both the baseline and CFL system cases, vehicle cabin soak is not included. Details of the configurations are listed in Table 3. The CFL system versus baseline system data are shown in Figure 16.

Table 3. CFL versus baseline configurations

Configuration	Cooling Mode	Heating Mode
Baseline System	Secondary loop A/C	PTC cabin heating PTC ESS heating
CFL System	Secondary loop A/C PEEM cooling ESS cooling	HP cabin heating HP ESS heating PEEM heat recovery

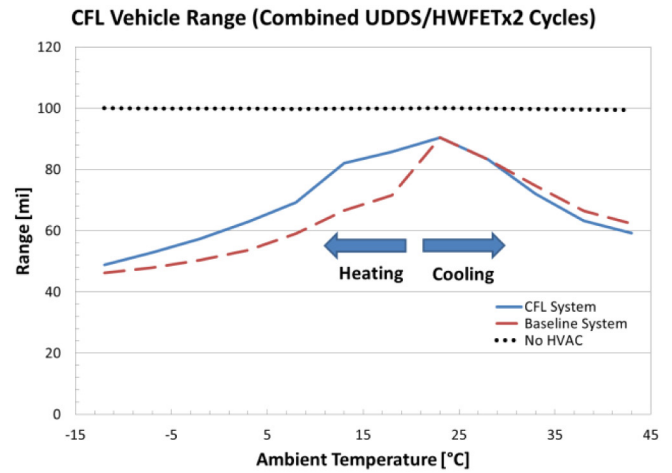


Figure 16. CFL versus baseline system for combined drive cycle vehicle range

It is apparent that the majority of the energy efficiency benefit of the CFL technology occurs in mild to moderate heating mode conditions. This is where the maximum benefit of the heat pump and PEEM waste heat recovery occurs. Another significant finding is that the CFL technology has little negative impact for mild cooling conditions up to 33°C. This is important to note because on a national level this is where the majority of cooling mode driving occurs and the moderate range loss at the extreme hot conditions have only a minor impact. It is also important to note that this is a comparison of the CFL technology with active ESS cooling to a baseline system without active ESS cooling, which is a conservative assumption because many EDVs already include active ESS cooling. This is critical because the energy consumption for active ESS cooling is the main source of the range difference between systems at the highest ambient temperatures, but that is where it is the most critical to ensuring battery cell longevity. If the CFL technology was compared to a baseline system that also included active battery cooling, the performance difference due to PEEM cooling would be minor.

When the national vehicle usage weighting was applied to the entire data set, the predicted vehicle range was 71.4 miles for the baseline case, and 77.8 miles for the CFL system. This is a 9.0% increase in predicted vehicle range at a national level. As a note of comparison the predicted vehicle range without using any thermal management system is 99.9 miles (not accounting for powertrain frictional loss or ESS capacity dependence on temperature). This means that the CFL system recovers 22.5% of the range that is lost due to operating the baseline system, i.e., it consumes 22.5% less energy than the baseline system to achieve the same thermal performance targets.

CONCLUSIONS

Experimental bench testing of the CFL technology has demonstrated both the feasibility of the approach and energy savings at a national level. The PEEM and ESS thermal demands were met by the CFL system under all of the drive cycles and ambient temperatures tested without the need for separate cooling loops. It was shown that incorporating the PEEM cooling system into the hot-side loop had only a minor negative impact on range during cooling conditions, typically below 1% and only under very hot weather conditions. During both mild cold and extreme cold weather, the PEEM waste heat recovery increased range by around 2%. Overall, the experimental, non-optimized CFL system showed an EDV range increase of 9% when weighted for U.S. national population and annual vehicle use, a 22.5% improvement over the experimental baseline. It is expected that an in-vehicle system will be capable of exceeding this 9% range increase when the components and control strategies are optimized for the application. There are no major remaining breakthroughs needed for the technology, and the next development stage will be vehicle-level demonstration by suppliers and vehicle manufacturers. In summary, bench testing of the CFL technology verified that EDV cooling loops can be combined to reduce the weight and volume of the system while providing the necessary thermal management of EDV subsystems and increasing vehicle range at a national level.

REFERENCES

1. Rugh, J., Pesaran, A., and Smith, K., "Electric Vehicle Battery Thermal Issues and Thermal Management Techniques," Presentation at SAE 2011 Alternative Refrigerant and System Efficiency Symposium, Scottsdale, AZ, Sept. 2011.
2. Bayerer, R., "Advanced Packaging Yields Higher Performance and Reliability in Power Electronics," *Microelectronics Reliability*, 50(9-11):1715-1719, 2010. doi:10.1016/j.microrel.2010.07.016.
3. Kamiya, M., Kawase, Y., Kosaka, T., and Matsui, N., "Temperature Distribution Analysis of Permanent Magnet in Interior Permanent Magnet Synchronous Motor Considering PWM Carrier Harmonics," presented at International Conference on Electrical Machines and Systems, Seoul, Korea, Oct. 2007.
4. Lohse-Busch, H., Duoba, M., Rask, E., and Meyer, M., *Advanced Powertrain Research Facility AVTA Nissan Leaf Testing and Analysis*. Argonne, IL: Argonne National Laboratory Report, Oct. 2012. http://www.transportation.anl.gov/D3/data/2012_nissan_leaf/AVTALeafTestingAnalysis_Major%20summary101212.pdf, accessed Feb. 2014.
5. Rugh, J. and Bennion, K., "Electric Vehicle Thermal Modeling to Assess Combined Cooling Loop Concepts," presented at SAE 2012 Thermal Management Systems Symposium, Scottsdale, AZ, Oct. 2012.
6. National Renewable Energy Laboratory, "Future Automotive Systems Technology Simulator," <http://www.nrel.gov/transportation/fastsim.html>, accessed Sept. 2013.
7. Gado, A., "Development of a Dynamic Test Facility for Environmental Control Systems" Ph.D. Dissertation, University of Maryland, 2006.
8. Santos, A.T., McGuckin, N., Nakamoto, H.Y., Gray, D., and Liss, S., *Summary of Travel Trends: 2009 National Household Travel Survey*. Report # FHWA-PL-11-022, U.S. Department of Transportation, June 2011.
9. Duthie, G., "Average Mobile A/C Customer Usage Model: Development and Recommendations," presented at SAE Automotive Alternate Refrigerant Systems Symposium, Scottsdale, AZ, July 2002.

CONTACT INFORMATION

Daniel Leighton
National Renewable Energy Laboratory
daniel.leighton@nrel.gov

ACKNOWLEDGMENTS

The author would like to thank Delphi and Halla Visteon Climate Control for material and engineering support. The author would also like to thank David Anderson and Lee Slezak in the Vehicle Technologies Office at the U.S. Department of Energy for sponsoring this work. Additional thanks to those at NREL who assisted with the project: Kevin Bennion, Cory Kreutzer, John Rugh, and Jeff Tomerlin.

DEFINITIONS/ABBREVIATIONS

A/C - air conditioning
CFL - combined fluid loop
Comp - compressor
EDV - electric-drive vehicle
EEV - electronic expansion valve
EM - electric motor
ESS - energy storage system
HP - heat pump
HVAC - heating, ventilation, and air conditioning
HWFET - Highway Fuel Economy Test
HX - heat exchanger
NREL - National Renewable Energy Laboratory
PE - power electronics
PEEM - power electronics and electric motor
PTC - positive temperature coefficient heater
RH - relative humidity
T - temperature
TEV - thermostatic expansion valve
UDDS - Urban Dynamometer Driving Schedule
Var - variable valve
WEG - water/ethylene glycol